JOURNAL OF BACTERIOLOGY, Oct. 1995, p. 5612–5621 Vol. 177, No. 19
0021-9193/95/$04.00+0

Mutations in Motif II of *Escherichia coli* DNA Helicase II Render the Enzyme Nonfunctional in Both Mismatch Repair and Excision Repair with Differential Effects on the Unwinding Reaction

ROBERT M. BROSH, JR.,[1] AND STEVEN W. MATSON[1,2]*

Department of Biology[1] and Curriculum in Genetics and Molecular Biology,[2] University of North Carolina, Chapel Hill, North Carolina 27599-3280

Received 8 May 1995/Accepted 20 July 1995

Site-directed mutagenesis has been employed to address the functional significance of the highly conserved aspartic and glutamic acid residues present in the Walker B (also called motif II) sequence in *Escherichia coli* DNA helicase II. Two mutant proteins, UvrDE221Q and UvrDD220NE221Q, were expressed and purified to apparent homogeneity. Biochemical characterization of the DNA-dependent ATPase activity of each mutant protein demonstrated a k_{cat} that was <0.5% of that of the wild-type protein, with no significant change in the apparent K_m for ATP. The E221Q mutant protein exhibited no detectable unwinding of either partial duplex or blunt duplex DNA substrates. The D220NE221Q mutant, however, catalyzed unwinding of both partial duplex and blunt duplex substrates, but at a greatly reduced rate compared with that of the wild-type enzyme. Both mutants were able to bind DNA. Thus, the motif II mutants E221Q and D220NE221Q were able to bind ATP and DNA to the same extent as wild-type helicase II but demonstrate a significant reduction in ATP hydrolysis and helicase functions. The mutant *uvrD* alleles were also characterized by examining their abilities to complement the mutator and UV light-sensitive phenotypes of a *uvrD* deletion mutant. Neither the *uvrDE221Q* nor the *uvrDD220NE221Q* allele, supplied on a plasmid, was able to complement either phenotype. Further genetic characterization of the mutant *uvrD* alleles demonstrated that *uvrDE221Q* confers a dominant negative growth phenotype; the *uvrDD220NE221Q* allele does not exhibit this effect. The observed difference in effect on viability may reflect the gene products' dissimilar kinetics for unwinding duplex DNA substrates in vitro.

Helicases catalyze the unwinding of duplex DNA, RNA, or DNA-RNA hybrids by disrupting the hydrogen bonds between complementary base pairs in an ATP hydrolysis-dependent reaction (19, 20, 24). These enzymes have essential roles in the processes of DNA replication, repair, recombination, transcription, and translation that are currently being elucidated (24, 26). At least 11 helicases have been identified in *Escherichia coli*, and many of these have been assigned functional roles in the cell. DNA helicase II, the product of the *uvrD* gene, is perhaps the most extensively characterized of these proteins. The enzyme is a DNA-dependent ATPase (36) and a 3′-to-5′ helicase (22). Helicase II prefers to unwind a double-stranded DNA (dsDNA) substrate in which a 3′ single-stranded DNA (ssDNA) tail is available for binding to initiate unwinding, but the enzyme can also initiate unwinding from a blunt end or a nick (37, 38). Helicase II has also been shown to unwind DNA-RNA hybrids with a 10-fold greater efficiency than duplex DNA (23). The macroscopic unwinding reaction mechanism exhibited by helicase II has been described as protein concentration dependent and leaves the ssDNA coated with helicase II (1, 15, 25, 37). In addition, the enzyme oligomerizes in solution, and the oligomer is stabilized by binding to DNA (39). Helicase II can also form a heterodimer with Rep protein upon binding DNA (47), although the physiological significance of this observation is still not clear.

Both genetic and biochemical data have demonstrated a role for helicase II in two DNA repair pathways, methyl-directed mismatch repair (10, 17, 31) and UvrABC-mediated nucleotide excision repair (4, 13, 33). Helicase II may also be involved in recombination (2, 21, 29, 32) and replication (7, 34), although the precise role played by the enzyme in these processes remains to be established.

Helicase II is a member of a family of proteins that share seven distinct regions of homology characterized by conserved amino acids (9, 11). Motifs I and II, previously identified as the Walker A and Walker B sequences, respectively, are conserved segments found in many nucleoside triphosphate (NTP)-binding proteins and all helicases characterized to date (8, 9, 44). Fry et al. (6) have demonstrated by nuclear magnetic resonance and X-ray diffraction analysis that motifs I and II are located near the MgATP binding site of adenylate kinase. Motif I consists of an α-helix containing two hydrophobic residues that interact with the adenine-ribose moiety of ATP and a lysine that may bind to the β and γ phosphates of ATP. Motif II contains a hydrophobic β-pleated sheet terminated by an aspartic acid that flanks the triphosphate chain of MgATP. These structural data suggest that motifs I and II are involved in nucleotide binding and/or hydrolysis. A site-specific mutation in motif I of helicase II, designated UvrDK35M, resulted in a mutant protein with a k_{cat} for DNA-dependent hydrolysis that was <0.5% of that of the wild-type protein and no significant change in the apparent K_m for ATP. This result suggests that the invariant lysine has a role in ATP hydrolysis but is not essential for binding of the nucleotide (7). The functions of the remaining five motifs are presently unknown.

The focus of the studies presented in this report was the highly conserved Walker B sequence that is found in ATP-binding proteins and referred to as motif II in DNA helicases. Site-directed mutagenesis was used to investigate the functional significance of the highly conserved acidic residues of motif II in DNA helicase II. Biochemical and genetic characterization of the mutant proteins was performed to understand

* Corresponding author. Mailing address: Dept. of Biology, CB# 3280, Coker Hall, University of North Carolina, Chapel Hill, NC 27599-3280. Phone: (919) 962-0005. Fax: (919) 962-1625.

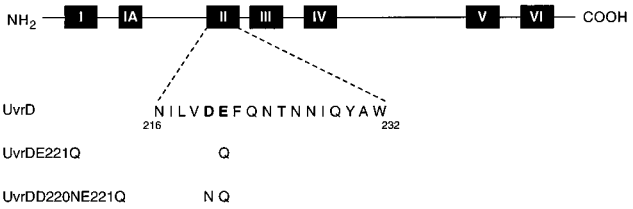

FIG. 1. Amino acid substitutions in motif II of DNA helicase II. The E221Q mutation in helicase II changes the highly conserved glutamic acid in the Walker ATPase B site to glutamine. The D220NE221Q mutation replaces both the aspartic acid and glutamic acid residues with asparagine and glutamine, respectively. The Walker B site is referred to as motif II in DNA and RNA helicases (9). The relative positions of the seven motifs in DNA helicase II are shown.

more fully the functional significance of motif II and the roles of helicase II in nucleic acid metabolism.

MATERIALS AND METHODS

Bacterial strains. *E. coli* BL21(DE3) (λDE3 *ompT* r_B^- m_B^-) and HMS174(DE3) (λDE3 *recA1* r^-_{K12} m^+_{K12} Rif^r) were obtained from Novagen. JH137 [K91 *lacZ dinD1*::MudI (Ap^r *lac*)] was obtained from P. Model. BL21(DE3)Δ*uvrD* and JH137Δ*uvrD* were previously constructed by V. Mendonca in this laboratory (7).

DNA and nucleotides. Bacteriophage M13mp18 and M13mp7 ssDNAs and their derivatives were prepared as described before (18). All unlabeled nucleotides were from U.S. Biochemicals Corp. except adenosine-5′-*O*-(3-thiotriphosphate), which was from Boehringer Mannheim. Plasmids pET9d and pET11d, which both contain T7 transcription-translation signals, were purchased from Novagen Inc. Concentrations of DNA and nucleotides were determined by UV spectrophotometry using published extinction coefficients and are expressed as nucleotide equivalents.

Enzymes. Restriction endonucleases, DNA polymerase I (large fragment), phage T7 DNA polymerase, and phage T4 polynucleotide kinase were purchased from New England Biolabs Inc. or U.S. Biochemical Corp. The reaction conditions were those suggested by the supplier. *E. coli* helicase II was purified from BL21(DE3)/pLysS cells containing the pET9d-H2wt expression plasmid (7). UvrDE221Q and UvrDD220NE221Q proteins were purified from BL21(DE3) Δ*uvrD*/pLysS cells containing the pET11d-H2E221Q and pET11d-H2D220N-E221Q expression plasmids. The procedure of Runyon et al. (39) was used to purify the wild-type and mutant proteins. Protein concentration was determined by using the helicase II extinction coefficient (39).

Site-directed mutagenesis and DNA constructions. A cassette containing the first 698 nucleotides of the *uvrD* gene, cloned in M13mp18, was the target for site-directed mutagenesis by published procedures (16, 49). Oligonucleotide 5′-TTCTGGAATTCGTTCACCAGGATA-3′ was used to alter codon 221 of *uvrD* from GAA (Glu) to CAA (Gln), and oligonucleotide 5′-TTCTGGAATT GGTTCACCAGGATA-3′ was used to alter codons 220 and 221 of *uvrD* from GACGAA (Asp-Glu) to AACCAA (Asn-Gln). The 698-nucleotide *Nco*I-*Bam*HI fragment with the site-specific mutation was then cloned into pET9d. The remaining portion of the *uvrD* gene and some 3′-flanking sequence was subsequently moved from M13mp18H2 as a *Bam*HI DNA fragment and ligated into pET9d containing the 698-nucleotide cassette. We were unable to construct the expression plasmid pET9d-H2D220N for technical reasons not understood at this time. The 2.5-kb *Nco*I-*Hin*dIII fragment, containing the entire *uvrD* gene, was moved from the pET9d construction into pET11d to yield pET11d-H2E221Q and pET11d-H2D220NE221Q. All mutations were verified by sequencing (41) of the complete *Nco*I-*Bam*HI cassette.

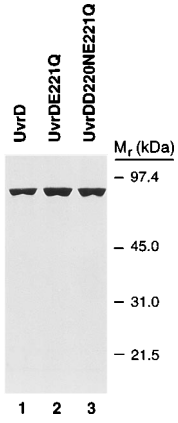

FIG. 2. Coomassie-stained 9.6% polyacrylamide–SDS gel of purified UvrD proteins. Wild-type and mutant polypeptides were purified as described in Materials and Methods. Lanes 1, 2, and 3 represent 1.848, 2.328, and 2.032 μg of UvrD, UvrDE221Q, and UvrDD220NE221Q proteins, respectively. The marker proteins were as follows: rabbit muscle phosphorylase b (97.4 kDa), hen egg white ovalbumin (45.0 kDa), bovine carbonic anhydrase (31.0 kDa), and soybean trypsin inhibitor (21.5 kDa).

TABLE 1. k_{cat} and K_m for DNA-dependent ATP hydrolysis catalyzed by UvrD, UvrDE221Q, and UvrDD220NE221Q[a]

Enzyme	k_{cat} (s^{-1})	K_m (μM)	k_{cat}/K_m (s^{-1} μM^{-1})
UvrD	75.9 ± 3.2	46.7 ± 2.6	1.6
UvrDE221Q	0.126 ± 0.021	16.0 ± 2.8	0.008
UvrDD220NE221Q	0.299 ± 0.032	133 ± 27	0.002

[a] Reaction conditions for DNA-dependent ATP hydrolysis assays were as described in Materials and Methods. For k_{cat} determinations, protein concentrations were 18.9, 237, and 207 nM for UvrD, UvrDE221Q, and UvrDD220NE221Q, respectively. The production of [^{3}H]ADP from [^{3}H]ATP was measured in a 30-μl reaction over a 5-min time course at 37°C. Aliquots (5 μl) were taken at 1-min intervals, and the rate of ATP hydrolysis was determined from linear plots of ADP production versus time. In a typical reaction, less than 20% of the ATP was hydrolyzed to minimize end product inhibition and substrate depletion effects. For K_m determinations, protein concentrations were 1.41, 355, and 310 nM for UvrD, UvrDE221Q, and UvrDD220NE221Q, respectively. Reaction mixtures (20 μl) for K_m determinations were incubated for 10 min at 37°C. The k_{cat} and K_m values measured for the DNA-dependent ATP hydrolysis reaction catalyzed by the UvrD proteins are the averages of at least three independent determinations.

Genetic assays. The viability of bacterial strains exposed to UV light was measured as follows. Overnight cultures of appropriate *E. coli* strains were used to innoculate 6 ml of LB medium (30) plus the appropriate antibiotic. Cells were grown to an optical density at 595 nm (OD_{595}) of 1, and 5 ml of each culture was centrifuged at 720 × *g* to collect the cell pellet. The cell pellet was resuspended in 10 ml of M9 minimal medium salts (30) and incubated at 37°C for 90 min under antibiotic selection to achieve the stationary phase. A 5-ml aliquot was removed and placed in a petri dish (60 by 15 mm). The cells were exposed to UV light at the indicated dosage and plated in the dark on plates containing LB agar plus antibiotic. Plates were incubated at 37°C for 24 to 36 h in the dark, and colonies were counted to calculate viability. Percent survival is expressed as the ratio of the viability of the cell strain at a specific UV light dose to the viability of the same unirradiated cell strain. The spontaneous mutation frequency for each cell strain was determined as described before (7).

DNA-binding assays. A nitrocellulose filter-binding assay was used to measure binding of UvrD proteins to DNA (28). Binding reaction mixtures (20 μl) contained 25 mM Tris-HCl (pH 7.5), 3 mM $MgCl_2$, 20 mM NaCl, 5 mM 2-mercaptoethanol, the 343-bp partial duplex helicase substrate (approximately 2 μM nucleotide phosphate) (85,000 cpm μmol^{-1}), 3 mM rATPγS, and the indicated amount of helicase II. The reaction mixture was incubated at 37°C for 10 min. The reaction mixture was then diluted with 1 ml of warmed (37°C) reaction buffer and passed over a nitrocellulose filter (0.45 μm; Whatman) at a flow rate of 4 ml/min. The filters were washed with 2 ml of warmed reaction buffer. The dried filters were counted in a liquid scintillation counter. Background radioactivity bound in the absence of UvrD protein was subtracted from total radioactivity bound to the filter. Nitrocellulose filters were pretreated by boiling in deionized distilled water for 20 min and stored in reaction buffer.

Helicase substrate preparation. The 343-bp M13mp7 partial duplex helicase substrate was constructed as described before (22). The 92-bp partial duplex substrate was constructed with a 90-mer oligonucleotide fragment complementary to positions 6142 to 6231 in M13mp7. The 90-mer was annealed to M13mp7 and labeled at its 3′ OH terminus with [α-^{32}P]dCTP as described before (22). The 20-bp partial duplex helicase substrate was constructed with a 20-mer oligonucleotide complementary to positions 7013 to 7032 in M13mp7. The oligonucleotide was labeled at its 5′ end with polynucleotide kinase and [γ-^{32}P]ATP as described before (40). The 20-mer was then annealed to M13mp7, and the mixture was applied to a 1-ml A5M spin column in a 1-ml syringe and spun at 2,000 rpm in a clinical centrifuge for 2 min. Material that flowed through the column was used directly as the helicase substrate. The 346-bp blunt-ended helicase substrate was constructed as described before (7).

Helicase assays. Helicase assay reaction mixtures (20 μl) contained 25 mM Tris-HCl (pH 7.5), 3 mM $MgCl_2$, 20 mM NaCl, 5 mM 2-mercaptoethanol, 3 mM rATP, and the indicated amount of helicase II. The concentration of the 343-,

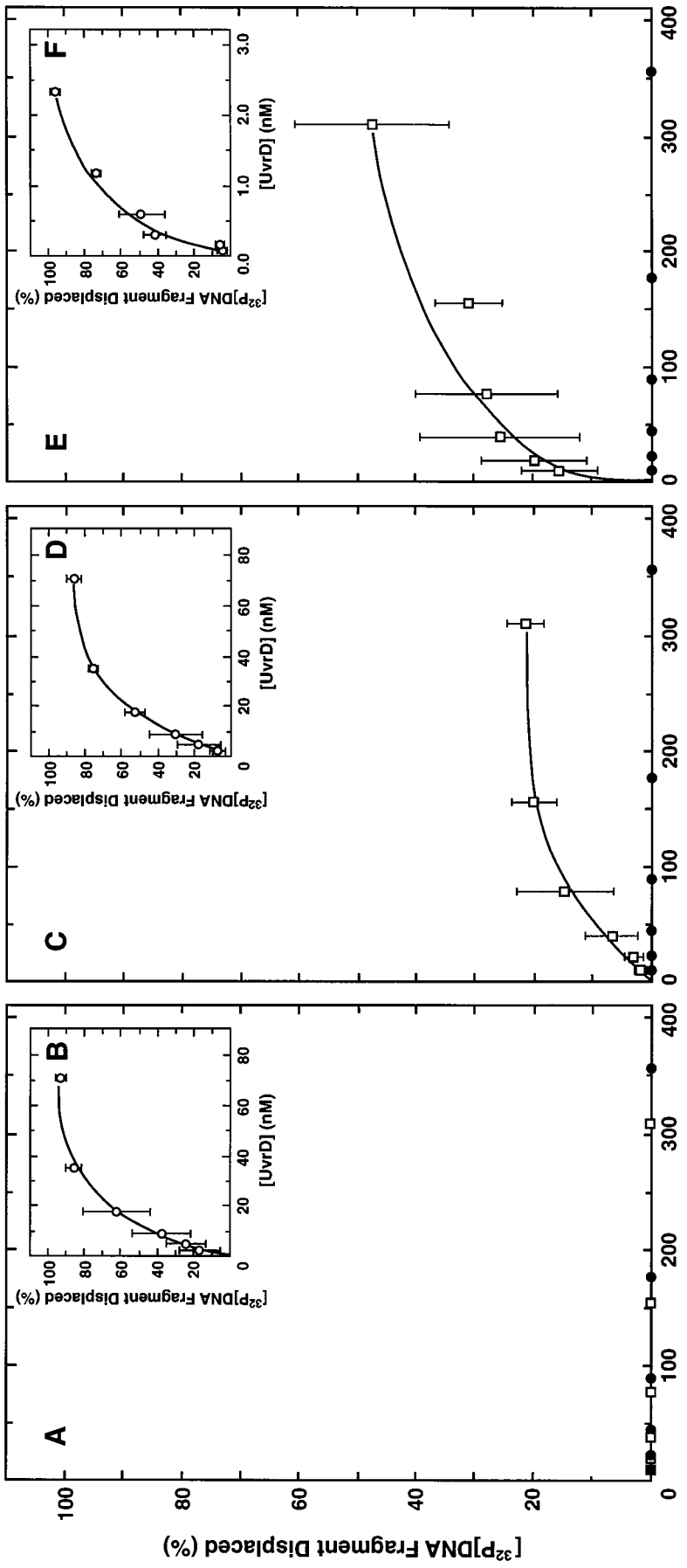

FIG. 3. Unwinding reaction catalyzed by the UvrDE221Q and UvrDD220NE221Q mutant proteins. Helicase reactions with partial duplex DNA substrates containing 343 bp of duplex DNA (A and B), 92 bp of duplex DNA (C and D), or 20 bp of duplex DNA (E and F) were done as described in Materials and Methods. Reactions were initiated by the addition of the indicated amounts of UvrDE221Q (●), UvrDD220NE221Q (□), or the wild-type enzyme (○) and incubated for 10 min at 37°C. The data presented represent the averages of three or more experiments.

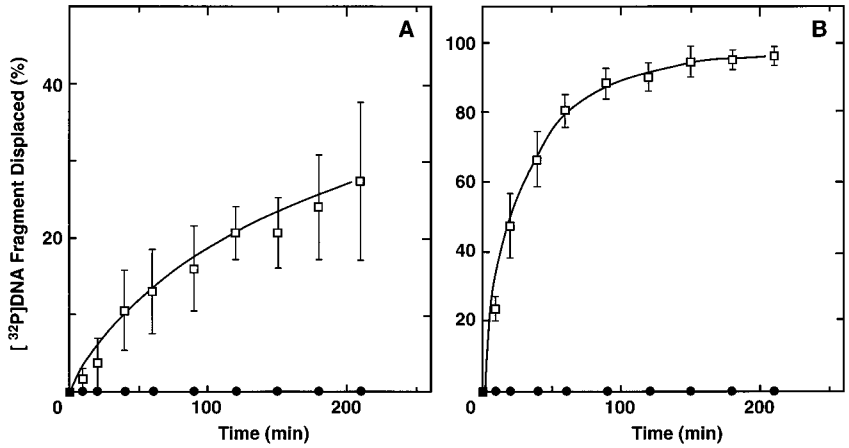

FIG. 4. UvrDD220NE221Q catalyzes a slow unwinding of partial duplex DNA substrates. Helicase reactions were done as described in Materials and Methods with either the 343-bp (A) or the 92-bp (B) partial duplex substrates with the following exceptions. Reaction mixtures were increased to 240 μl, and a 20-μl aliquot was removed at time zero. The reaction was initiated by the addition of UvrDE221Q at a final concentration of 355 nM (monomer) (●) or UvrDD220NE221Q at a final concentration of 310 nM (monomer) (□), and incubation was done at 37°C. Aliquots (20 μl) were removed at the indicated times and analyzed by polyacrylamide gel electrophoresis as described in Materials and Methods. The data presented represent the averages of at least three independent experiments.

92-, and 20-bp partial duplex helicase substrates in the reaction mixtures was approximately 2 μM (nucleotide phosphate). The concentration of the 346-bp substrate in the assay was approximately 0.5 μM (nucleotide phosphate). Reactions were initiated by the addition of ATP and incubated at 37°C for 10 min. Reactions were terminated by the addition of 10 μl of 50 mM EDTA–40% glycerol–0.5% sodium dodecyl sulfate (SDS)–0.1% bromophenol blue–0.1% xylene cyanol. The products of helicase reactions with the 343-, 92-, and 20-bp partial duplex substrates were resolved on 6, 8, and 12% nondenaturing polyacrylamide gels, respectively, as described before (25). The products of the helicase reaction with the 346-bp fully duplex substrate were separated on a 6% nondenaturing polyacrylamide gel as described before (7). Polyacrylamide gels were imaged and quantified by phosphor storage technology and software (Molecular Dynamics).

DNA-dependent ATPase assays. The hydrolysis of ATP to ADP was measured as previously described (27). ATPase reaction mixtures were identical to helicase reaction mixtures except that they contained M13mp7 ssDNA (9 μM nucleotide phosphate) and [^{3}H]ATP (22 cpm/pmol). For k_{cat} determinations, the [^{3}H]ATP concentration was 540 μM. For K_m determinations, the [^{3}H]ATP concentration ranged between 25 and 500 μM.

RESULTS

The Walker B sequence, also referred to as motif II, is a highly conserved region found in ATP-binding proteins that include prokaryotic and eukaryotic DNA and RNA helicases. Aspartic acid 220 and glutamic acid 221 of helicase II are very highly conserved amino acid residues located within the ATPase B site originally described by Walker et al. (44). To further our understanding of the functional role of motif II in DNA helicases, two specific mutations were made in the well-characterized UvrD protein from *E. coli* (Fig. 1). The single substitution E221Q replaces the highly conserved glutamic acid at position 221 with a glutamine. This isosteric substitution removes the negative charge and replaces it with a neutral amino acid. The double substitution D220NE221Q replaces the highly conserved aspartic and glutamic acids at positions 220 and 221, respectively, with an asparagine and glutamine, respectively. The mutant proteins were expressed and purified to apparent homogeneity (Fig. 2).

Biochemical characterization of UvrDE221Q and UvrDD220NE221Q. The ssDNA-dependent ATPase, helicase, and ssDNA-binding activities of the mutant proteins were measured and compared with the activities of the wild-type protein. The ATP hydrolysis kinetic constants k_{cat} and K_m are shown in Table 1. The k_{cat} values of UvrDE221Q and UvrDD220NE221Q were 0.126 and 0.299 s^{-1}, determined to be approximately 0.2 and 0.4% of that of the wild-type protein, respectively. No significant change in the apparent K_m for ATP was detected for either mutant protein compared with wild-type UvrD. The specificity constant (k_{cat}/K_m) was reduced 100-fold for both mutant proteins. This reduction can be attributed to a dramatic decrease in the k_{cat} value, with little change in the K_m value indicating that Glu-221 is involved in the ATP hydrolysis reaction catalyzed by helicase II and apparently is not essential for the binding of ATP.

We also examined the unwinding activity of the mutant proteins with both partial duplex and blunt duplex DNA substrates. Titrations of the UvrD, UvrDE221Q, and UvrDD220NE221Q proteins with partial duplex DNA substrates are shown in Fig. 3. Wild-type helicase II, at a concentration of 17.7 nM (monomer), unwound 62% of the 343-bp partial duplex DNA substrate in a 10-min reaction (Fig. 3B). No detectable unwinding of this substrate could be observed at concentrations of

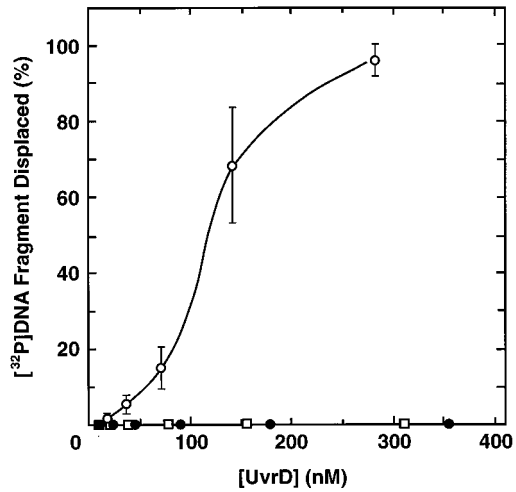

FIG. 5. Unwinding reaction on a blunt duplex DNA substrate catalyzed by UvrD, UvrDD220NE221Q, and UvrDE221Q. Helicase reactions with a 346-bp blunt duplex DNA substrate were done as described in Materials and Methods. Reactions were initiated by the addition of the indicated amounts of UvrDE221Q (●), UvrDD220NE221Q (□), or the wild-type enzyme (○) and incubated for 10 min at 37°C.

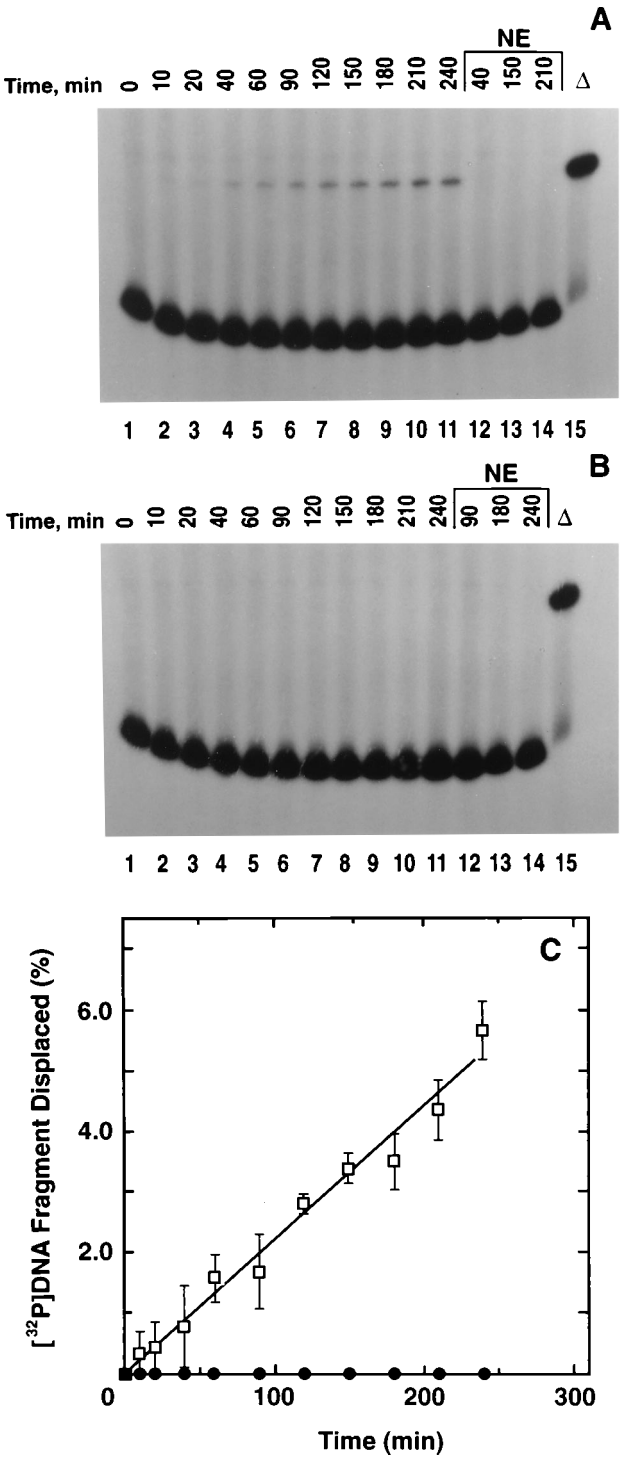

FIG. 6. UvrDE221Q protein fails to catalyze an unwinding reaction on a blunt duplex DNA substrate. Helicase reactions were done as described in Materials and Methods with the 346-bp blunt duplex DNA substrate with the following exceptions. Reaction mixtures were increased to 240 μl, and a 20-μl aliquot was removed at time zero. The reaction was initiated by the addition of UvrDE221Q at a final concentration of 355 nM (monomer) or UvrDD220NE221Q at a final concentration of 310 nM (monomer), and incubation was at 37°C. Aliquots were removed at the indicated times and analyzed by polyacrylamide gel electrophoresis as described in Materials and Methods. Note that fully denatured ssDNA migrates above the duplex DNA substrate. The data presented represent the averages of at least three independent experiments. (A) Aliquots were removed from the reaction mix after UvrDD220NE221Q enzyme was added at the indicated times and analyzed by nondenaturing gel electrophoresis (lanes 1 to 11). Lanes 12 to 14 represent 20-μl aliquots removed from a 240-μl reaction in which enzyme was omitted and analyzed as described. Lane 15 is a heat-denatured control. An autoradiograph from a typical helicase assay is shown. (B) Aliquots were removed from the reaction mix after UvrDE221Q enzyme was added at the indicated times and analyzed by nondenaturing gel electrophoresis (lanes 1 to 11). Lanes 12 to 14 represent 20-μl aliquots removed from a 240-μl reaction in which enzyme was omitted and analyzed as described. Lane 15 is a heat-denatured control. An autoradiograph from a typical helicase assay is shown. (C) Quantitative data from several experiments as shown in panel A (□) and panel B (●).

E221Q and D220NE221Q of up to 355 and 310 nM (monomer), respectively (Fig. 3A). With a 92-bp partial duplex substrate, wild-type helicase II at 17.7 nM (monomer) displaced 53% of the 92-mer (Fig. 3D). The UvrDD220NE221Q protein at a concentraion of 310 nM (monomer) unwound 21% of the 92-mer (Fig. 3C). No unwinding of the 92-bp partial duplex substrate could be detected with UvrDE221Q at concentrations of up to 355 nM (monomer). Wild-type UvrD protein at 1.17 nM (monomer) unwound approximately 73% of the 20-bp partial duplex substrate (Fig. 3F). UvrDD220NE221Q at 310 nM (monomer) unwound 48% of the 20-bp partial duplex (Fig. 3E). Again, we detected no unwinding catalyzed by UvrDE221Q up to a concentration of 355 nM (monomer).

A kinetic analysis of the unwinding reaction catalyzed by UvrDD220NE221Q demonstrated a relatively linear increase in the fraction of the 343-bp duplex unwound during a 210-min incubation (Fig. 4A). At this time point, approximately 27% of the substrate had been unwound. The UvrDE221Q protein failed to unwind the 343-bp partial duplex even when reaction mixes were incubated for up to 210 min. When the 92-bp partial duplex substrate was used, UvrDD220NE221Q unwound 95% of the DNA substrate, whereas UvrDE221Q (178 nM) again exhibited no unwinding of the substrate after an extended reaction (Fig. 4B). Thus, UvrDD220NE221Q is capable of unwinding both long and short partial duplex substrates, albeit at a greatly lower rate than wild-type UvrD. UvrDE221Q, on the other hand, failed to catalyze unwinding of any DNA substrate that we tested.

Helicase II has also been shown to unwind blunt-ended duplex DNA substrates (38). We tested the ability of both UvrD mutant proteins to unwind a 346-bp blunt duplex (Fig. 5). Wild-type helicase II, at a concentration of 150 nM (monomer), unwound approximately 68% of the 346-bp fragment in a 10-min reaction. No detectable unwinding of the 346-bp blunt duplex substrate could be observed at concentrations of UvrDE221Q and UvrDD220NE221Q of up to 355 and 310 nM (monomer), respectively. We also examined the blunt duplex DNA-unwinding reaction catalyzed by the mutant proteins at various points during a 210-min incubation (Fig. 6). UvrDD220NE221Q unwound up to 6% of the 346-bp DNA fragment in a time-dependent reaction (Fig. 6A). UvrDE221Q failed to unwind the 346-bp blunt duplex substrate even after extended incubation (Fig. 6B and C).

The marked reduction in the DNA-dependent ATP hydrolysis and helicase reactions catalyzed by the two mutant proteins led us to examine their DNA-binding properties with the 92-bp partial duplex substrate (Fig. 7). In the presence of the poorly hydrolyzed ATP analog adenosine 5′-*O*-thiotriphosphate, both UvrDE221Q and UvrDD220NE221Q demonstrated a binding isotherm similar to that measured for the wild-type enzyme. Similar binding of the mutant and wild-type proteins to DNA was also observed in the presence of ATP or ADP (data not shown). Thus, both UvrDE221Q and UvrDD220NE221Q are able to bind DNA, suggesting that

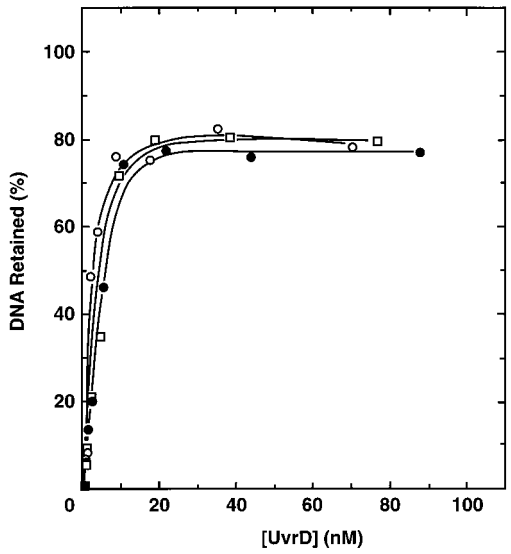

FIG. 7. Motif II mutants bind DNA. Binding assays were performed as described in Materials and Methods with the indicated amounts of UvrD (○), UvrDE221Q (●), or UvrDD220NE221Q (□). Background values were typically less than 2% and have been subtracted from the reported data. These data represent the averages of at least three independent determinations.

the reduction in DNA-dependent ATP hydrolysis and helicase activity is not due to an inability to interact with DNA.

***uvrDE221Q* allele exhibits a dominant negative growth phenotype.** To begin a genetic characterization of the two mutant *uvrD* alleles, plasmids containing *uvrD* (pET9d-H2wt), *uvrDE221Q* (pET9d-H2E221Q), and *uvrDD220NE221Q* (pET9d-H2D220NE221Q) were transformed into *E. coli* HMS174 and HMS174(DE3). Expression of the relevant *uvrD* gene is driven by the T7 RNA polymerase promoter in these constructions, and the T7 RNA polymerase gene is present on the lambda DE3 lysogen in HMS174(DE3). Expression of T7 RNA polymerase in this cell strain is regulated by the isopropylthiogalactopyranoside (IPTG)-inducible *lacUV5* promoter. Since the *lacUV5* promoter is never fully repressed, the level of T7 RNA polymerase present in HMS174(DE3), in the absence of induction, can be significant. Evidence for uninduced expression of T7 RNA polymerase, and therefore the plasmid-borne gene, has been provided by Western (immunoblot) analysis, demonstrating that helicase II expression from the uninduced pET9d-H2wt plasmid is approximately the same as that from the chromosome of HMS174(DE3) (7).

Transformation efficiencies for each plasmid in several cell strains are shown in Table 2. The transformation efficiency of pET9d-H2E221Q and pET9d-H2D220NE221Q was reduced below detectable limits in HMS174(DE3) in the absence of IPTG-induced expression of the T7 RNA polymerase gene. Thus, a basal level of expression of *uvrDE221Q* or *uvrDD220NE221Q* is toxic in a lambda DE3 lysogen. The wild-type gene does not exhibit this toxicity. To inhibit the T7 RNA polymerase expressed in the absence of induction, we introduced a second plasmid, either pLysS or pLysE. These plasmids carry the gene encoding T7 lysozyme, which inhibits T7 RNA polymerase. A higher level of expression of the T7 lysozyme gene is achieved with the pLysE plasmid. Therefore, in uninduced cells containing the lambda DE3 lysogen, the relative activity of T7 RNA polymerase is HMS174(DE3) > HMS174(DE3)/pLysS > HMS174(DE3)/pLysE. Consequently, expression of the plasmid-borne helicase II gene should be greatest in HMS174(DE3) and lowest in HMS174(DE3)/pLysE in the absence of IPTG induction. The data demonstrate that a plasmid carrying the *uvrDE221Q* allele cannot stably transform HMS174(DE3)/pLysS or pLysE. It is evident that even modest expression of the *uvrDE221Q* allele is lethal in a cell containing a wild-type chromosomal copy of the *uvrD* gene. These results are in contrast to the data obtained with pET9d-H2D220NE221Q, where transformants were recovered in the pLysS and pLysE backgrounds. Thus, the *uvrDD220NE221Q* allele exhibits a less toxic dosage effect on the cell than the *uvrDE221Q* allele.

To more directly demonstrate that the *uvrDE221Q* allele conferred a dominant negative growth phenotype, pET11d-H2E221Q was transformed into HMS174(DE3)/pLysE to construct a conditionally lethal mutant strain. The pET11d vector contains the Lac repressor-binding site immediately downstream of the bacteriophage T7 ϕ10 promoter to further reduce the uninduced expression of the cloned gene. In addition, this plasmid contains a copy of the *lacI* gene to ensure adequate production of the Lac repressor. Cells harboring a plasmid containing either a wild-type copy of the *uvrD* gene, *uvrDD220NE221Q*, or *uvrDE221Q* were grown at 37°C for 60 min, and IPTG was added to induce expression of the plasmid-encoded copy of the *uvrD* gene. At the indicated times, cells were plated, in the absence of IPTG, to determine cell viability (Fig. 8). Within 60 min after the addition of IPTG, there was a threefold decrease in the number of viable cells expressing the UvrDE221Q mutant protein (Fig. 8B). Viability decreased to 0.04% of that of the control culture by 2 h after IPTG addition. Cells expressing UvrDD220NE221Q showed a slight decrease in viability 120 min after IPTG induction and a more pronounced decrease by 150 min after IPTG induction (Fig. 8C). Cells expressing wild-type UvrD protein exhibited only a modest decrease in growth rate 120 min after IPTG induction compared with the control culture (Fig. 8A).

Mutant alleles fail to complement DNA repair pathways. Helicase II has a direct role in the UvrABC-mediated nucleotide excision repair pathway (4, 13, 33). To assess the ability of UvrDE221Q and UvrDD220NE221Q to function in this pathway, we determined the relative UV sensitivity of various strains expressing the mutant proteins (Fig. 9). Neither *uvrDE221Q* nor *uvrDD220NE221Q*, supplied on a plasmid, was capable of complementing the UV-sensitive phenotype exhibited by the *uvrD* deletion strain JH137Δ*uvrD*. The UV-sensitive phenotype of JH137Δ*uvrD* was complemented by the presence of the wild-type *uvrD* allele supplied on the same

TABLE 2. Plasmid transformation efficiency[a]

Strain	Transformation efficiency (CFU/ng of DNA)			
	pET9d	pET9d-H2wt	pET9d-H2E221Q	pET9d-H2D220N-E221Q
HMS174	174 ± 144	140 ± 86	141 ± 131	73 ± 32
HMS174(DE3)	152 ± 97	17 ± 12	<0.37[b]	<0.37[b]
HMS174(DE3)/pLysS	288 ± 205	254 ± 163	<0.37[b]	85 ± 62
HMS174(DE3)/pLysE	350 ± 301	89 ± 79	<0.37[b]	233 ± 183

[a] Approximately 10^8 competent cells were transformed with 32 ng of the indicated $CsCl_2$-purified plasmid. An aliquot (0.10 ml) of a 1.2-ml transformation mixture was plated on kanamycin (30 μg/ml) or kanamycin and chloramphenicol (30 μg/ml each) plates. Both 0.1 and 1.1 ml of the transformation mixture was plated for pET9d, pET9d-H2wt, pET9d-H2E221Q, and pET9d-H2D220NE221Q transformations. These transformation efficiencies represent the averages of at least three independent experiments.

[b] No transformants were recovered. This value represents the sensitivity of the assay. The actual transformation efficiency may be much lower.

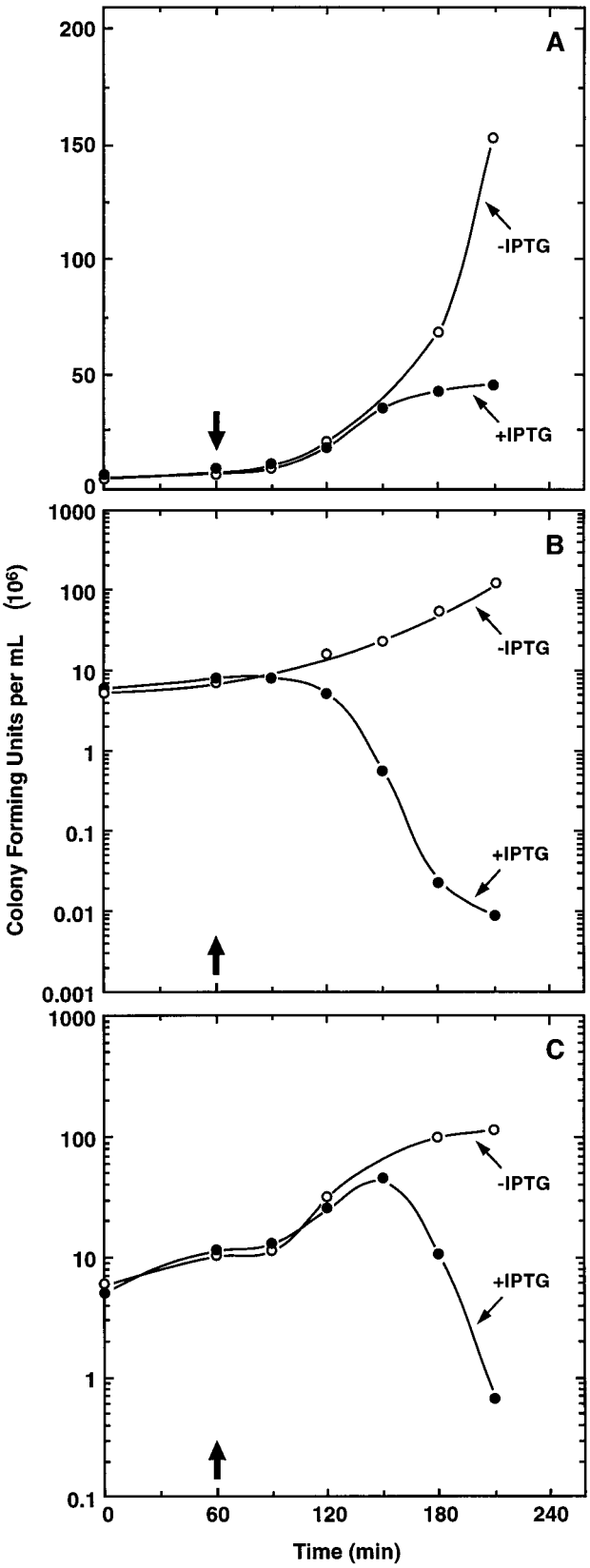

FIG. 8. *uvrDE221Q* allele exhibits a dominant lethal phenotype. Fresh overnight cultures of HMS174(DE3)/pLysE/pET11d-H2wt (A), HMS174(DE3)/pLysE/pET11d-H2E221Q (B), and HMS174(DE3)/pLysE/pET11d-H2D220NE221Q (C) were diluted 1:200 into 20 ml of fresh LB medium containing the appropriate antibiotics and incubated at 37°C with constant shaking. Aliquots were removed at the indicated times, serially diluted, and plated on LB plates containing the appropriate antibiotics to obtain viable-cell counts. IPTG (50 μM) was added to one of two duplicate cultures at the 60-min time point, as indicated by the arrow. The data presented are typical of one of three independent experiments.

expression plasmid. These results suggest that the ATPase and/or helicase activities of helicase II are required in excision repair. Interestingly, JH137Δ*uvrD*/pET9d-H2E221Q exhibited a reproducible hypersensitivity to UV light. The effect was most dramatic at UV doses of 18 and 24 J/m^2 at which the viability of JH137Δ*uvrD*/pET9d-H2E221Q was approximately 10-fold less than that of JH137Δ*uvrD*.

The UvrDE221Q and UvrDD220NE221Q mutant proteins were also examined for their abilities to function in methyl-directed mismatch repair. The mutant allele was introduced into a *uvrD* deletion strain on a plasmid, and the spontaneous mutation frequencies of JH137Δ*uvrD*/pET9d-H2E221Q, JH137-Δ*uvrD*/pET9d-H2D220NE221Q, and JH137Δ*uvrD*/pET9d-H2wt at the *rpoB* locus were measured and compared with those of relevant strains, as shown in Table 3. The relative mutability values of JH137Δ*uvrD*/pET9d-H2E221Q, JH137Δ*uvrD*/pET9d-H2D220NE221Q, and JH137Δ*uvrD*/pET9d-H2wt were found to be 62, 149, and 2.36, respectively. Thus, *uvrDE221Q* and *uvrD-D220NE221Q* failed to complement JH137Δ*uvrD* in methyl-directed mismatch repair, whereas the wild-type *uvrD* allele expressed from the same plasmid exhibits complementation. We conclude that UvrDE221Q and UvrDD220NE221Q do not function in methyl-directed mismatch repair. The mutation frequencies of JH137 (a strain with a wild-type copy of *uvrD* on the chromosome) transformed with pET9d-H2wt, pET9d-H2D220N-E221Q, and pET9d-H2E221Q were also measured and found to be equivalent to that of JH137. Thus, neither *uvrDE221Q* nor *uvrDD220NE221Q* exhibits a phenotype in the presence or absence of wild-type helicase II with regard to mismatch repair.

DISCUSSION

To better understand the functional significance of the motif II region found in DNA helicases, we have mutagenized the most conserved residues of the segment, Asp-220 and Glu-221, in the *E. coli* UvrD protein. These two acidic residues, residing at the C-terminal end of a β strand, constitute a portion of the nucleotide-binding pocket found in all helicases identified to date. The impact of motif II site-specific mutations on the biochemical activities and genetic functions of helicase II was evaluated.

The highly conserved residue Glu-221 of helicase II is required for catalytic efficiency in both the ATPase and helicase reactions. Replacement of Glu-221 by a glutamine resulted in a 500-fold decrease in the k_{cat} for ssDNA-dependent ATP hydrolysis. The apparent K_m for ATP remained approximately the same. These results demonstrate that the single substitution of glutamine for the highly conserved glutamic acid severely compromised the ATP hydrolysis activity of the enzyme but did not significantly alter the binding affinity of the enzyme for ATP. The results presented here are similar to those obtained in other biochemical studies of RNA helicase eIF-4A (35) and DNA helicase NS-1 (14), in which mutation of the conserved acidic residues in motif II decreased ATPase activity, with little impact on ATP binding. The E221Q mutant also failed to unwind partial duplex DNA substrates ranging from 20 to 343 bp in length, as well as a blunt duplex substrate 346 bp in length. To address the possibility that the reduction in ssDNA-dependent ATPase and helicase activities was due to a defect in DNA binding, the DNA-

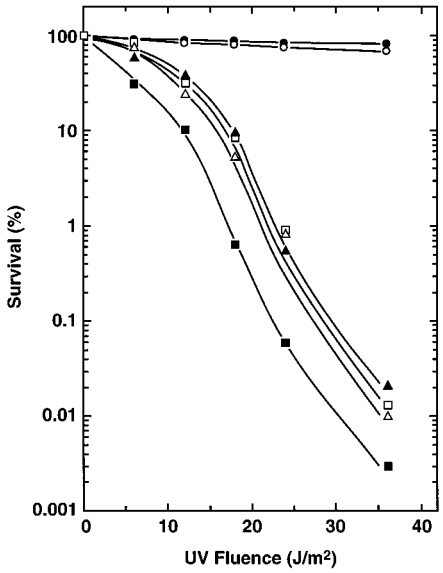

FIG. 9. UV light sensitivity of JH137 and JH137 derivatives. Cell strains JH137 (●), JH137Δ*uvrD* (▲), JH137Δ*uvrD*/pET9d (△), JH137Δ*uvrD*/pET9d-H2wt (○), JH137Δ*uvrD*/pET9d-H2E221Q (■), and JH137Δ*uvrD*/pET9d-H2D220NE221Q (□) were irradiated with UV light as described in Materials and Methods. Data (percent survival) are expressed as the number of UV-irradiated cells forming colonies as a fraction of the colonies formed by unirradiated cells and represent the averages of three independent experiments.

binding activity of both mutant and wild-type proteins was examined. The E221Q mutant retains DNA-binding activity similar to that of wild-type UvrD. Therefore, the drastically reduced ATPase and helicase activity of UvrDE221Q is not due to an impaired interaction with DNA. The inability of UvrDE221Q to unwind even a short 20-bp DNA duplex likely reflects the low k_{cat} for ATP hydrolysis, since the two activities are believed to be directly coupled.

The UvrDD220NE221Q mutant also demonstrated a significant reduction in the k_{cat} for ATP hydrolysis, with little change in the apparent K_m for ATP. In addition, this protein bound DNA. Surprisingly, the UvrDD220NE221Q mutant retained a measurable unwinding activity on partial duplex as well as blunt duplex DNA substrates, although the unwinding activity was markedly reduced compared with that of the wild-type enzyme. The fact that this mutant retained some unwinding activity may reflect the k_{cat} for ATP hydrolysis, which was approximately twofold higher than that measured for UvrDE221Q. The double substitution mutant may retain just enough ATPase activity to support a weak helicase reaction. Taken together, these data suggest that the highly conserved acidic residues in motif II are involved in the ATP hydrolysis reaction catalyzed by helicase II. These residues are apparently not essential for ATP binding. The data are also consistent with the notion that the ATPase and helicase activities are directly coupled. In fact, the results may begin to define a minimum level of ATPase activity required to support the unwinding reaction. At present we do not understand why the introduction of a second amino acid change, which results in the removal of both negatively charged amino acids, partially restores unwinding activity to the inactive E221Q mutant. Perhaps there is some subtle change in tertiary structure that permits a slightly higher level of ATP hydrolysis. This, in turn, might fuel a very limited helicase reaction. Knowledge of the crystal structure of the protein will likely be required to fully understand these results.

Analysis of motif II mutants in other helicases has demonstrated that the effects of amino acid substitutions on enzymatic activity are not always predictable. Mutation of the translation initiation factor eIF-4A motif II sequence from DEAD to EEAD resulted in only a 20% reduction in ATPase activity, with a dramatic reduction in RNA helicase activity (35). Mutagenesis of the second E to Q in the motif II E-E pair in nucleoprotein NS-1 resulted in a 99% reduction in ATPase activity, whereas a K replacement resulted in just a 12% reduction in ATPase activity (14). It is interesting that both mutations in NS-1 substantially decreased DNA helicase activity. In general, motif II mutations have an impact on the ATPase and helicase activities of both RNA and DNA helicases. Many of these mutations dramatically affect catalytic activity. Thus, motif II seems to be directly involved in the DNA-dependent ATPase reaction and indirectly involved in the helicase reaction. It is also clear that motif II mutations do not impact DNA binding, suggesting that motif II does not play a direct role in DNA binding. It should be noted that the impact of these mutations on binding of protein to ssDNA versus dsDNA cannot be determined because of the nature of the partial duplex DNA substrate used in the DNA-binding assays.

The biochemical characterization of the mutant proteins has been complemented with genetic experiments to further probe the function of the UvrD protein in the cell. We examined the ability of the two mutant proteins to participate in DNA repair pathways by measuring their abilities to complement JH137-Δ*uvrD* in either methyl-directed mismatch repair or nucleotide excision repair. Neither mutant was functional in either pathway. Thus, both of these repair pathways require the ATPase and/or helicase activities of helicase II. It is important that the

TABLE 3. Mutation frequencies of JH137 and JH137 derivatives

Strain	Relevant genotype	Mutation frequency (10^{-8})[a]	Relative mutability
JH137	*uvrD*$^+$	2.64 ± 1.19[b]	1
JH137Δ*uvrD*	Δ*uvrD*	448 ± 165[b]	169
JH137Δ*uvrD*/pET9d-H2wt	*uvrD*$^+$	6.24 ± 4.41[b]	2.36
JH137Δ*uvrD*/pET9d-H2E221Q	*uvrDE221Q*	164 ± 85.1	62
JH137Δ*uvrD*/pET9d-H2D220NE221Q	*uvrDD220NE221Q*	393 ± 72.3	149
JH137/pET9d-H2E221Q	*uvrD*$^+$/*uvrDE221Q*	2.11 ± 1.97	0.80
JH137/pET9d-H2D220NE221Q	*uvrD*$^+$/*uvrDD220NE221Q*	1.72 ± 0.086	0.65

[a] Mutation frequency was determined by dividing the number of resistant colonies formed on selective agar by the total number of cells plated. Relative mutability values were obtained by dividing the mutation frequency of the cell strain in question by the frequency of the wild-type strain.

[b] Value previously determined in this lab (7).

UvrDD220NE221Q mutant, which did catalyze a slow unwinding reaction, was not able to substitute for helicase II in either repair pathway. This suggests that the minimal helicase activity retained by this enzyme was not sufficient to support the excision of short oligonucleotides containing pyrimidine dimers or the longer DNA tracts replaced in methyl-directed mismatch repair. These results provide some insight into the repair phenotypes of another *uvrD* mutation, *uvrD252*. *E. coli uvrD252* strains are defective in recombination and excision repair but functional in methyl-directed mismatch repair in vivo (5, 12, 43, 45). The purified *uvrD252* gene product exhibits reduced ATPase and helicase activity in vitro (46) but appears to have greater catalytic activity than UvrDD220NE221Q, although the reaction conditions were different. This enzymatic difference may account for the nearly normal level of methyl-directed mismatch repair exhibited by *uvrD252* compared with the deficiency in mismatch repair demonstrated by *uvrDD220NE221Q*. If this is the case, then the UV sensitivity of cells harboring *uvrDE221Q*, *uvrDD220NE221Q*, or *uvrD252* suggests that excision repair requires a helicase II molecule with greater catalytic activity than does methyl-directed mismatch repair.

It is interesting that JH137Δ*uvrD*/pET9d-H2E221Q exhibited a greater sensitivity to UV light than did JH137Δ*uvrD*. We can suggest two possible explanations for this observation. First, the basal level of UvrABC-mediated nucleotide excision repair, in the absence of helicase II, is further impaired by a stalled mutant helicase II oligomer at the lesion. An inactive complex at the lesion could prevent oligonucleotide excision, DNA polymerase I recognition, and/or the turnover of repair proteins UvrB and C. Second, another pathway for repair of DNA damage caused by UV light has been blocked by the catalytically inactive UvrDE221Q protein. For example, postreplication recombinational repair fills gaps left when DNA polymerase III bypasses a DNA lesion during replication. A number of genes encode proteins involved in postreplication repair, including *uvrD* and *rep* (3, 42, 48). It has been demonstrated in vitro that helicase II can form a homodimer (39) or a heterodimer with Rep protein upon binding DNA (47). Perhaps Rep protein is inactivated when complexed with UvrDE221Q, effectively blocking a pathway of postreplication repair. Further characterization of the biochemical interactions between helicase subunits and the genetic roles of helicase multimers should provide insight into such possibilities.

In addition to the repair phenotypes discussed above, there is a dominant negative growth phenotype associated with the expression of the *uvrDE221Q* allele in a wild-type cell. Previous analysis by Western blotting has demonstrated that the uninduced expression of a *uvrD* gene from pET9d-H2wt in HMS174(DE3) is approximately the same as *uvrD* expression from the chromosome (7). Thus, expression of the *uvrDE221Q* allele at a ratio of about 1:1 with the wild-type *uvrD* allele results in a dominant negative growth phenotype, as evidenced by the inability to recover transformants when HMS174(DE3), HMS174(DE3)/pLysS, and HMS174(DE3)/pLysE were transformed with pET9d-H2E221Q. Similar results were obtained previously with another allele encoding a catalytically inactive protein, UvrDK35M (7). The use of an IPTG-inducible plasmid, pET11d-H2E221Q, allowed construction of a conditionally lethal cell strain. Cells expressing UvrDE221Q showed a marked reduction in cell viability within 60 min after protein expression was derepressed. Cells expressing the *uvrDD220NE221Q* allele exhibited a decrease in viability that was not nearly as dramatic as that of cells expressing *uvrDE221Q*. Moreover, transformants were obtained in the HMS174(DE3)/pLysS and pLysE backgrounds with the pET9d-H2D220NE221Q plasmid. Cells expressing the plasmid-encoded wild-type *uvrD* allele exhibited only a reduction in growth rate 2 h after IPTG induction. Lethality due to overproduction of helicase II has been reported (39) but is not likely to be responsible for the result reported here, since cells expressing the wild-type *uvrD* gene remain viable. Expression of UvrDE221Q and UvrDD220NE221Q impacts viability differently, perhaps reflecting the very different unwinding activities of the two mutant proteins. The slow unwinding reaction catalyzed by UvrDD220NE221Q may fulfill a basic function required of the UvrD protein. Perhaps a dimer formed between a UvrDD220NE221Q monomer and a wild-type monomer is less defective than a UvrDE221Q–wild-type helicase II dimer. Alternatively, UvrDD220NE221Q may fail to interact with or inactivate some other cellular protein, presumably by oligomerization, leaving the cellular protein able to perform its function in the cell. A possible candidate for such an interaction is Rep protein, which forms a heterodimer with helicase II upon binding DNA (47). The fact that *uvrD rep* double deletion mutants are not viable suggests that helicase II and/or Rep protein may function in an essential pathway, such as replication (45). It is possible that UvrDE221Q negatively impacts cell viability by inactivating Rep protein or some other essential protein. Further work will be required to distinguish among these possibilities.

ACKNOWLEDGMENTS

We thank Tim Lohman, Ken Marians, and Jim George for critical reading of the manuscript. We are grateful to Susan Whitfield for preparation of the artwork.

This investigation was supported in part by National Institutes of Health grant GM33476 (to S.W.M.).

REFERENCES

1. **Abdel-Monem, M., H. Durwald, and H. Hoffman-Berling.** 1977. DNA unwinding enzyme II of *Escherichia coli*: characterization of the DNA unwinding activity. Eur. J. Biochem. **79:**39–45.
2. **Arthur, H. M., and R. G. Lloyd.** 1980. Hyper-recombination in *uvrD* mutants of *Escherichia coli* K12. Mol. Gen. Genet. **180:**185–191.
3. **Bridges, B. A., and A. Wright.** 1981. Influence of mutations at the *rep* gene on survival of *Escherichia coli* following ultraviolet light irradiation or 8-methoxypsoralen photosensitization. Mutat. Res. **82:**229–238.
4. **Caron, P. R., S. R. Kushner, and L. Grossman.** 1985. Involvement of helicase II (*uvrD* gene product) and DNA polymerase I in excision mediated by the UvrABC protein complex. Proc. Natl. Acad. Sci. USA **82:**4925–4929.
5. **Feinstein, S. I., and K. B. Low.** 1986. Hyper-recombining recipient strains in bacterial conjugation. Genetics **113:**13–33.
6. **Fry, D. C., S. A. Kuby, and A. S. Mildran.** 1986. ATP-binding site of adenylate kinase: mechanistic implications of its homolog with *ras*-encoded p21, F_1-ATPase, and other nucleotide-binding proteins. Proc. Natl. Acad. Sci. USA **83:**907–911.
7. **George, J. W., R. M. Brosh, Jr., and S. W. Matson.** 1994. A dominant negative allele of the *Escherichia coli uvrD* gene encoding DNA helicase II: a biochemical and genetic characterization. J. Mol. Biol. **235:**424–435.
8. **Gorbalenya, A. E., and E. V. Koonin.** 1990. Superfamily of UvrA-related NTP-binding proteins: implications for rational classification of recombination/repair systems. J. Mol. Biol. **213:**583–591.
9. **Gorbalenya, A. E., E. V. Koonin, A. P. Donchenko, and V. M. Blinov.** 1988. A novel superfamily of nucleoside triphosphate-binding motif containing proteins which are probably involved in duplex unwinding in DNA and RNA replication and recombination. FEBS Lett. **235:**16–24.
10. **Grilley, M., L. Holmes, B. Yashar, and P. Modrich.** 1990. Mechanisms of DNA-mismatch correction. Mutat. Res. **236:**253–267.
11. **Hodgman, T. C.** 1988. A new superfamily of replicative proteins. Nature (London) **333:**22–23.
12. **Horii, Z. L., and A. J. Clark.** 1973. Genetic analysis of the *RecF* pathway to genetic recombination in *Escherichia coli* K12: isolation and characterization of mutants. J. Mol. Biol. **80:**327–344.
13. **Husain, I., B. Van Houten, D. C. Thomas, and M. Abdel-Monem.** 1985. Effect of DNA polymerase I and DNA helicase II on the turnover rate of UvrABC excision nuclease. Proc. Natl. Acad. Sci. USA **82:**6774–6778.
14. **Jindal, H. K., C. B. Yong, G. M. Wilson, P. Tam, and C. R. Astell.** 1994. Mutations in the NTP-binding motif of minute virus of mice (MVM) NS-1 protein uncouple ATPase and DNA helicase functions. J. Biol. Chem. **269:** 3283–3289.

15. **Kuhn, B., M. Abdel-Monem, H. Krell, and H. Hoffman-Berling.** 1979. Evidence for two mechanisms of DNA unwinding catalyzed by DNA helicases. J. Biol. Chem. **254:**11343–11350.
16. **Kunkel, T. A., K. Bebenek, and J. McClary.** 1991. Efficient site-directed mutagenesis using uracil-containing DNA. Methods Enzymol. **204:**125–139.
17. **Lahue, R. S., K. G. Au, and P. Modrich.** 1989. DNA mismatch correction in a defined system. Science **245:**160–164.
18. **Lechner, R. L., and C. C. Richardson.** 1983. A preformed, topologically stable replication fork. J. Biol. Chem. **258:**11185–11196.
19. **Lohman, T. M.** 1993. Helicase-catalyzed DNA unwinding. J. Biol. Chem. **268:**2269–2272.
20. **Lohman, T. M.** 1992. *Escherichia coli* DNA helicases: mechanisms of DNA unwinding. Mol. Microbiol. **6:**5–14.
21. **Maples, V. F., and S. R. Kushner.** 1982. DNA repair in *Escherichia coli*: identification of the *uvrD* gene product. Proc. Natl. Acad. Sci. USA **79:**5616–5620.
22. **Matson, S. W.** 1986. *Escherichia coli* DNA helicase II (*uvrD* gene product) translocates unidirectionally in a 3′-5′ direction. J. Biol. Chem. **261:**10169–10175.
23. **Matson, S. W.** 1989. *Escherichia coli* DNA helicase II (*uvrD* gene product) catalyzes the unwinding of DNA-RNA hybrids in vitro. Proc. Natl. Acad. Sci. USA **86:**4430–4434.
24. **Matson, S. W., D. W. Bean, and J. W. George.** 1994. DNA helicases: enzymes with essential roles in all aspects of DNA metabolism. Bioessays **16:**13–22.
25. **Matson, S. W., and J. W. George.** 1987. DNA helicase II of *Escherichia coli*. J. Biol. Chem. **264:**17502–17512.
26. **Matson, S. W., and K. A. Kaiser-Rogers.** 1990. DNA helicases. Annu. Rev. Biochem. **59:**289–329.
27. **Matson, S. W., and C. C. Richardson.** 1983. DNA-dependent nucleoside 5′-triphosphatase activity of the gene 4 protein of bacteriophage T7. J. Biol. Chem. **258:**14009–14016.
28. **Matson, S. W., and C. C. Richardson.** 1985. Nucleotide-dependent binding of the gene 4 protein of bacteriophage T7 to single-stranded DNA. J. Biol. Chem. **260:**2281–2287.
29. **Mendonca, V. M., K. A. Kaiser-Rogers, and S. W. Matson.** 1993. Double helicase II (*uvrD*)-helicase IV (*helD*) deletion mutants are defective in the recombination pathways of *Escherichia coli*. J. Bacteriol. **175:**4641–4651.
30. **Miller, J. H.** 1972. Experiments in molecular genetics, p. 431–433. Cold Spring Harbor Laboratory, Cold Spring Harbor, N.Y.
31. **Modrich, P.** 1989. Methyl-directed DNA mismatch correction in a defined system. J. Biol. Chem. **264:**6597–6600.
32. **Morel, P., J. A. Hejna, S. D. Ehrlich, and E. Cassuto.** 1993. Antipairing and strand transferase activities of *Escherichia coli* helicase II (*uvrD*). Nucleic Acids Res. **21:**3205–3209.
33. **Orren, D. K., C. P. Selby, and A. Hearst.** 1991. Post-incision steps of nucleotide excision repair in *Escherichia coli*. J. Biol. Chem. **267:**780–788.
34. **Ossanna, N., and D. W. Mount.** 1989. Mutations in *uvrD* induce the SOS response in *Escherichia coli*. J. Bacteriol. **171:**303–307.
35. **Pause, A., and N. Sonenberg.** 1992. Mutational analysis of a DEAD box RNA helicase: the mammalian translation initiation factor eIF-4A. EMBO J. **11:**2643–2654.
36. **Richet, E., and M. Kohiyama.** 1976. Purification and characterization of a DNA-dependent ATPase from *Escherichia coli*. J. Biol. Chem. **251:**808–812.
37. **Runyon, G. T., D. G. Bear, and T. M. Lohman.** 1990. *Escherichia coli* helicase II (UvrD) protein initiates DNA unwinding at nicks and blunt ends. Proc. Natl. Acad. Sci. USA **87:**6383–6387.
38. **Runyon, G. T., and T. M. Lohman.** 1989. *Escherichia coli* helicase II (UvrD) can completely unwind fully duplex linear and nicked circular substrates. J. Biol. Chem. **264:**17502–17512.
39. **Runyon, G. T., I. Wong, and T. M. Lohman.** 1993. Overexpression, purification, and dimerization of *uvrD* gene product (helicase II). Biochemistry **32:**602–612.
40. **Sambrook, J., E. F. Fritsch, and T. Maniatis.** 1989. Molecular cloning: a laboratory manual, 2nd ed., p. 5.68–5.69. Cold Spring Harbor Laboratory, Cold Spring Harbor, N.Y.
41. **Sanger, F., S. Nicklen, and A. R. Coulson.** 1977. DNA sequencing with chain terminating inhibitors. Proc. Natl. Acad. Sci. USA **74:**5463–5467.
42. **Sargentini, N. J., and K. C. Smith.** 1980. Involvement of genes *uvrD* and *recB* in separate deoxyribonucleic acid repair pathways in *Escherichia coli* K-12 *uvrB5* and B/R *uvrA155*. J. Bacteriol. **143:**212–220.
43. **Siegel, E. C., and H. Race.** 1981. Phenotypes of UV-sensitive *uvrD3*, *recL152*, and *uvrE15* mutants of *Escherichia coli*. Mutat. Res. **83:**49–59.
44. **Walker, J. M., M. Sarsate, M. J. Runswick, and N. J. Gay.** 1982. Distantly related sequences in the A and B-subunits of ATP synthase, myosin, kinases, and other ATP-requiring enzymes and a common nucleotide binding fold. EMBO J. **1:**945–951.
45. **Washburn, B. K., and S. R. Kushner.** 1991. Construction and analysis of deletions in the structural gene (*uvrD*) for DNA helicase II of *Escherichia coli*. J. Bacteriol. **178:**2569–2575.
46. **Washburn, B. K., and S. R. Kushner.** 1993. Characterization of DNA helicase II from *uvrD252* mutant of *Escherichia coli*. J. Bacteriol. **175:**341–350.
47. **Wong, I., M. Amaratunga, and T. M. Lohman.** 1993. Heterodimer formation between *Escherichia coli* Rep and UvrD proteins. J. Biol. Chem. **268:**20386–20391.
48. **Youngs, D. A., and K. C. Smith.** 1976. Genetic control of multiple pathways of postreplicational repair in *uvrB* strains of *Escherichia coli* K-12. J. Bacteriol. **125:**102–110.
49. **Zoller, M. J., and M. Smith.** 1989. Oligonucleotide-directed mutagenesis of DNA fragments cloned into M13 vectors, p. 537. *In* R. Wu, L. Grossman, and K. Moldave (ed.), Recombinant DNA methodology. Academic Press, San Diego.